UDK 621.791:621.791.053:669.14.018.8
Review article/Pregledni članek

ISSN 1580-2949
MTAEC9, 47(4)403(2013)

EFFECT OF HEAT TREATMENT ON THE MICROSTRUCTURE AND MECHANICAL PROPERTIES OF MARTENSITIC STAINLESS-STEEL JOINTS WELDED WITH AUSTENITIC STAINLESS-STEEL FILLERS

VPLIV TOPLOTNE OBDELAVE NA MIKROSTRUKTURO IN MEHANSKE LASTNOSTI MARTENZITNIH NERJAVNIH SPOJEV, VARJENIH Z AVSTENITNIMI NERJAVNIMI ELEKTRODAMI

Adnan Calik, Mustafa Serdar Karakaş

Department of Manufacturing Engineering, Faculty of Technology, Suleyman Demirel University, 32260 Cunur, Isparta, Turkey
adnancalik@sdu.edu.tr

Prejem rokopisa – received: 2012-11-08; sprejem za objavo – accepted for publication: 2013-01-04

AISI 422 martensitic stainless steels were welded according to the ISO 15792-1 standard with austenitic stainless-steel filler. The effects of tempering and preheating heat treatments were also evaluated. The microstructures of the welds were characterized with optical microscopy. Mechanical properties were determined via microhardness, tensile and fatigue tests, and compared to those of the unwelded AISI 422 steel. X-ray diffraction was used to characterize the phases present in the weld. Chromium carbides were observed at the grain boundaries of the welds. The precipitation was caused mainly by the diffusion of carbon into the austenitic stainless steel during the welding. The microhardness decreased from the base metal to the weld. The tensile-strength and percent-elongation values were improved with preheating and tempering heat treatments. The highest fatigue limit was obtained with preheating.

Keywords: welding, heat treatment, stainless steel, fatigue, hardness

Martenzitno nerjavno jeklo AISI 422 je bilo varjeno skladno s standardom ISO 15792-1 z elektrodami iz avstenitnega nerjavnega jekla. Ocenjen je bil vpliv kaljenja in predogrevanja. Mikrostruktura zvarov je bila opredeljena s svetlobno mikroskopijo. Mehanske lastnosti so bile določene z mikrotrdoto, nateznimi in utrujenostnimi preizkusi in primerjane z nevarjenim jeklom AISI 422. Rentgenska difrakcija je bila uporabljena za karakterizacijo faz v zvaru. Po mejah zrn v zvaru je bilo opaziti kromove karbide. Večino izločanja je povzročila difuzija ogljika v avstenitno jeklo med varjenjem. Mikrotrdota se je zmanjševala od osnovnega materiala do zvara. Vrednosti natezne trdnosti in delež raztezka so se povečali s predgrevanjem in s toplotno obdelavo. Najvišja odpornost proti utrujanju je bila dosežena s predgrevanjem.

Ključne besede: varjenje, toplotna obdelava, nerjavno jeklo, utrujenost, trdota

1 INTRODUCTION

For metals, fatigue failures occur more often in welded joints than in unwelded structures. Weld defects and imperfections affect the fatigue and other mechanical properties of structures.[1,2] In general, fatigue strength decreases significantly with the introduction of any stress raisers in metals. Machine parts contain stress raisers in industrial applications. Fatigue cracks in structural parts almost always initiate at geometrical irregularities.[3]

Weld defects and imperfections can be accepted as critical stress raisers in welded structures. Fatigue properties of welded joints are more complicated because of the nature of the weld. Slag inclusions, pores, undercuts, incomplete fusion and residual stresses all affect the crack initiation and crack-propagation stages of the fatigue life of a welded joint.[4–6] In addition, surface roughness and section changes may also affect the existing or newly developing fatigue cracks. The fatigue behavior of a welded joint is influenced by the thickness of a plate as well as by the other geometrical parameters.[7] However, there is conflicting evidence with regard to the effect of a welding procedure on the fatigue strength. For the fillet-welded and butt-welded joints the fatigue strength is strongly dependent on the welding procedure.[8,9]

In spite of a poor weldability, martensitic stainless steels may be welded in the annealed, stress-relieved and tempered conditions. As an alloying element, Cr has very significant effects on the metallurgical aspect of the martensitic stainless steels. Cr and C are specifically added to steel to ensure the formation of martensite after the hardening. Ni can be added, and it enhances both the yield strength and ductility of these steels. The hardness in this type of material is dependent on the carbon content.[10] The carbon content can also affect the hardness of the heat-affected zone (HAZ). Thus, the influence of hardness of HAZ may be controlled with welding characteristics. In general, the welding of the martensitic stainless steels with a carbon content higher than 0.25 % is not recommended. In the 0.05–0.15 % C range, the hardness increases with the increasing carbon concentration. Austenitic or ferritic-austenitic electrodes are used for martensitic stainless steels. The hardness and ductility of a weld and HAZ vary in a welded structure. To avoid this harmful effect on the welded AISI 420

Table 1: Chemical composition of the AISI 422 steel in mass fractions, *w*/%
Tabela 1: Kemijska sestava jekla AISI 422 v masnih deležih, *w*/%

Element	C	Si	S	P	Mn	Ni	Cr	Mo	V	Fe
Composition	0.220	0.220	0.023	0.02	0.403	1.268	11.15	0.086	0.017	Bal.

steel, preheating and a slow cooling rate after the welding must be considered.[11,12]

In this study, an attempt has been made to clarify the effects of pre- and post-weld treatments on the welding of the martensitic stainless steel with an austenitic stainless-steel filler. The present study highlights the effects of preheating and tempering on the microstructural, hardness and tensile properties, and on the fatigue behavior of the welded joints.

2 EXPERIMENTAL PROCEDURE

2.1 Materials

AISI 422 steel in its annealed state was used as the base metal for the welding experiments. The chemical composition of the steel is given in **Table 1**. This steel is widely used in the transmission systems of diesel locomotives. Cylindrical as-cast billets of 80 mm diameters and 1 m lengths were hot-forged at 800 °C into the plates of 25 mm thickness.

The forged plates were then machined to the weld specimen dimensions specified in the ISO 15792-1 standard. The geometry of the weld specimens is shown in **Figure 1a**. Type 1.3 specimens were used and their dimensions are given in **Table 2**. An OFHC (Oxygen Free High Conductivity) copper backing strip was used during the welding. The sequence of the welding passes is shown in **Figure 1b**.

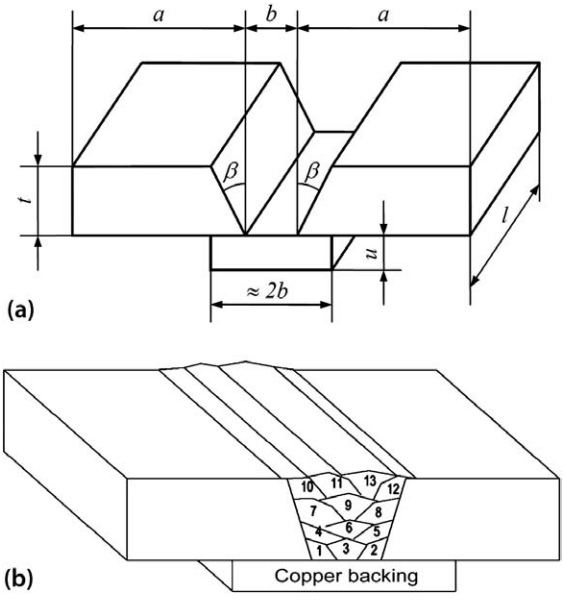

Figure 1: a) Shape and dimensions of a weld specimen as indicated in the ISO 15792-1 standard; b) sequence of the welding passes
Slika 1: a) Oblika in dimenzije varjenih vzorcev, kot je prikazano v ISO 15792-1 standardu, b) potek zaporedja prehodov v zvaru

Table 2: Dimensions (mm) of the type 1.3 weld test specimen depicted in **Figure 1**
Tabela 2: Dimenzije (mm) preizkušanca za varjenje vrste 1.3, prikazanega na **sliki 1**

t	*a*	*b*	*u*		*l*
20	≥ 150	16	6	10	≥ 150

The specimens were thoroughly cleaned with acetone before the welding. The austenitic stainless-steel electrodes (E310L) of a 3.25 mm diameter were used for the welding tests. The chemical composition of the welding electrodes is shown in **Table 3**. In order to prevent hydrogen-induced cracking, the electrodes were dried in a muffle furnace at 573 K for 2 h before the welding. The welding procedure was then carried out manually in a single V-butt-joint configuration using a UMS 250 DC type electric-arc welding machine with a total of 13 passes. The current was held constant at 170 A. The total of 13 runs were needed to fill the groove between the butt joints.

Table 3: Chemical composition of the E310L filler electrode in mass fractions, *w*/%
Tabela 3: Kemijska sestava varilne elektrode E310L v masnih deležih, *w*/%

C	Mn	Si	Ni	Cr	Fe
0.10	2.0	0.4	20	25	Bal.

The effects of preheating and tempering heat treatments were investigated. The welding parameters and notations used for the as-welded, preheated and tempered specimens are summarized in **Table 4**. From here onwards, the codes AW, PH and TP shall be used to express the as-welded, preheated and tempered specimens, respectively.

Table 4: Welding parameters used for the test specimens
Tabela 4: Parametri varjenja, uporabljeni pri preizkusnih vzorcih

Specimen	Filler metal	Preheating	PWHT
AW	E310L	N/A	N/A
PH	E310L	623 K, 2 h	N/A
TP	E310L	N/A	1023 K, 3 h

2.2 Metallography

The microstructures of the welded joints were evaluated using optical microscopy. The specimens examined were prepared using standard metallographic techniques. The original microstructure of the original AISI 422 steel (before the welding) is shown in **Figure 2**. This reveals a fine, fully martensitic microstructure.

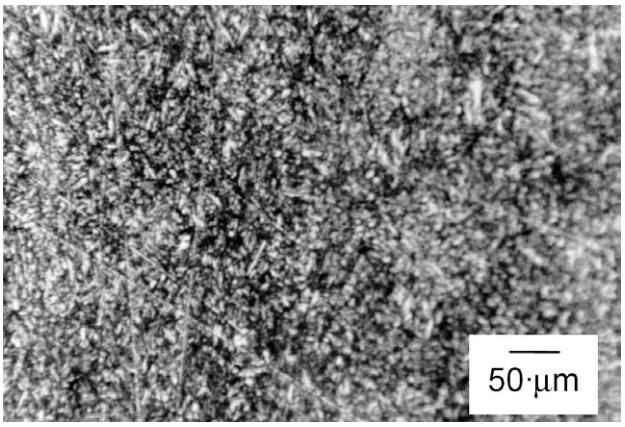

Figure 2: Microstructure of the AISI 422 base metal
Slika 2: Mikrostruktura osnovnega materiala AISI 422

2.3 Mechanical testing

Tensile, fatigue, and microhardness test specimens were extracted from the welded samples. Tensile tests were carried out at room temperature in accord with the ISO 6892-1 standard. Yield strength (YS), ultimate tensile strength (UTS) and fraction of elongation (% EL) values were determined. Fatigue tests were done using a rotating bar bending fatigue testing machine in accord with the ISO 1143-1 standard. Microhardness measurements were made utilizing a Vickers indenter with a load of 100 g and dwell time of 15 s. For each of the mechanical tests, a minimum of three measurements/tests were made for each experimental condition.

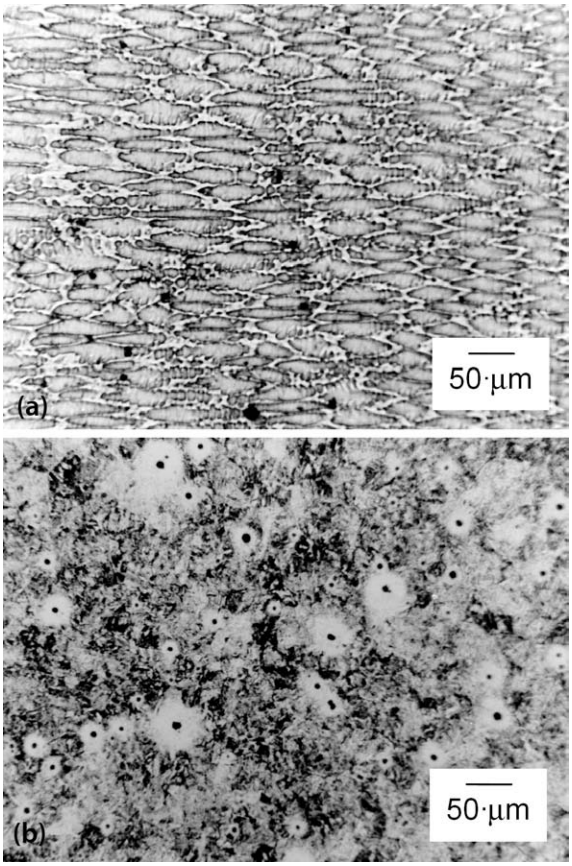

Figure 3: Microstructure of the AW specimen: a) weld metal; b) HAZ
Slika 3: Mikrostruktura AW-vzorcev: a) zvar, b) toplotno vplivana cona (HAZ)

3 RESULTS AND DISCUSSION

After the welding, the specimens generally consisted of three distinctive regions: (i) the weld metal; (ii) the heat-affected zone (HAZ) and (iii) the base metal that was not affected by the welding process. The microstructures of the AW specimen are shown in **Figure 3**. The weld metal shows a microstructure consisting mainly of austenite (**Figure 3a**), with delta ferrite present at the grain boundaries.

The HAZ of the AW specimen revealed both martensite and austenite phases. The coexistence of the two phases in the AW specimen is shown in **Figure 3b**. The microstructure also shows the presence of precipitates (possibly inclusions) located at the centers of the austenite phases. The XRD pattern of the weld in **Figure 4** indicates the presence of chromium carbides ($Cr_{23}C_6$, Cr_7C_3). High temperatures, combined with the diffusion of C from the martensitic stainless steel to the austenitic stainless steel may have caused the formation of these carbides during the welding.

The microstructures of the PH specimen are shown in **Figure 5**. The microstructure of the weld metal reveals an austenitic structure with possible delta ferrite segregated at the grain boundaries (**Figure 5a**). The heat affected zone (HAZ) between the weld and the base metal reveals the presence of martensite and austenite phases (**Figure 5b**).

The microstructures of the TP specimen are shown in **Figure 6**. The microstructure of the weld metal is austenitic, similar to the weld metal observed in the AW and PH specimens. However, the dendritic morphology of the austenitic structure is much more visible (**Figure 6a**).

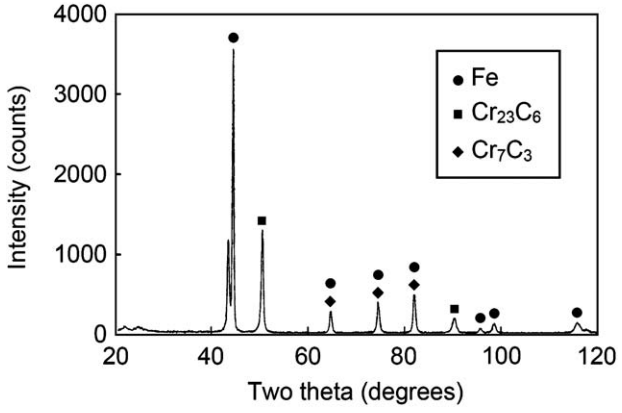

Figure 4: XRD pattern of the AW specimen indicating the presence of chromium carbides
Slika 4: Rentgenski (XRD) posnetek, ki kaže prisotnost kroma v vzorcu AW

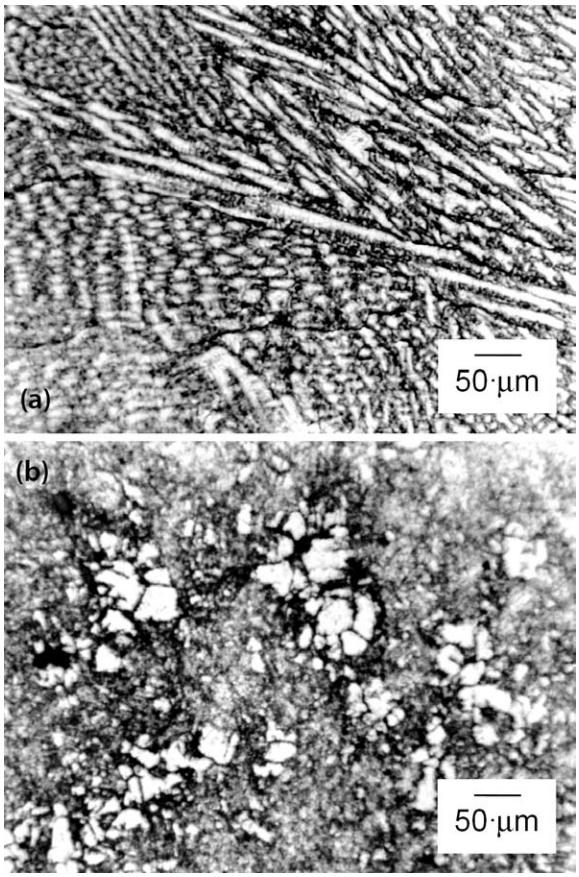

Figure 5: Microstructure of the PH specimen: a) weld metal; b) HAZ
Slika 5: Mikrostruktura PH-vzorca: a) zvar, b) toplotno vplivana cona (HAZ)

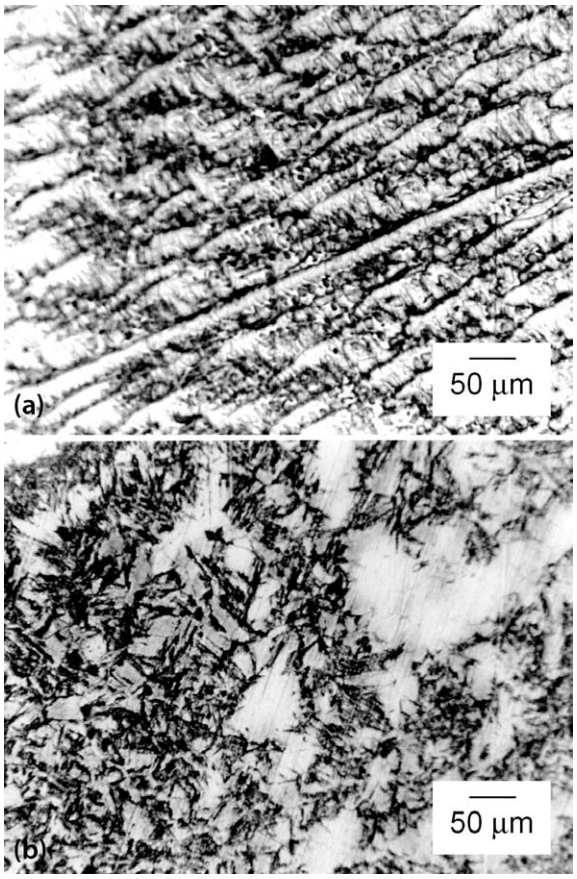

Figure 6: Microstructure of the TP specimen: a) weld metal; b) HAZ
Slika 6: Mikrostruktura TP-vzorca: a) zvar, b) toplotno vplivana cona (HAZ)

The heat affected zone (HAZ) between the weld and the base metal again reveals a microstructure consisting of martensite and austenite phases (**Figure 6b**). Compared to the AW and PH specimens, the martensite phase in the TP specimen has a coarser appearance due to the effects of tempering.

The hardness test results are summarized in **Figure 7**. Microhardness measurements were made both across and along the weld centerline. **Figure 7a** indicates a decrease in the microhardness towards the weld metal for all the welded joints. This is expected, since the base metal consists of martensite and the weld metal consists of either austenite or a mixture of austenite and some delta ferrite. **Figure 7b** shows the microhardness distribution for the weld from top to bottom. While the microhardness distribution for the AW specimen is more or less constant, a steady decrease is observed for the PH and TP specimens. As welding was carried out in 13 passes, each pass resulted in a tempering treatment on the previous pass, which led to the softening of the underlying layers.

The tensile-test results for the welded specimens are listed in **Table 5**. Failures occurred within the weld metal. The YS showed no change with preheating and remained constant at 490 MPa. The tempering treatment

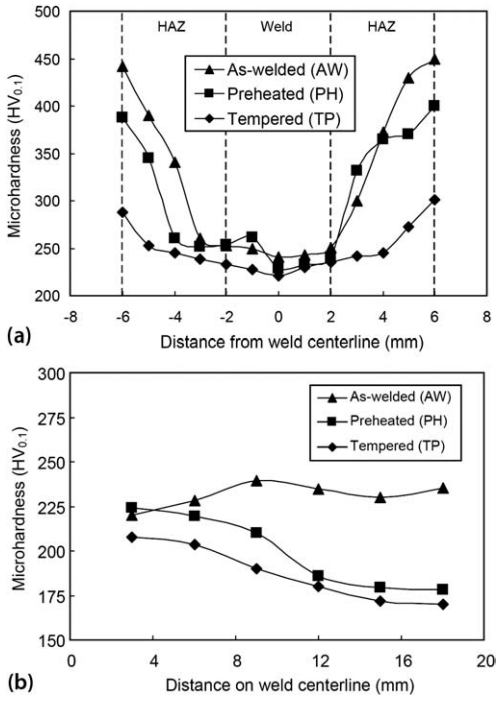

Figure 7: Microhardness distribution for the welded joints: a) across the weld centerline and b) on the weld centerline from top to bottom
Slika 7: Razporeditev mikrotrdote v varjenih spojih: a) preko sredine zvara in b) na sredini zvara od vrha do dna

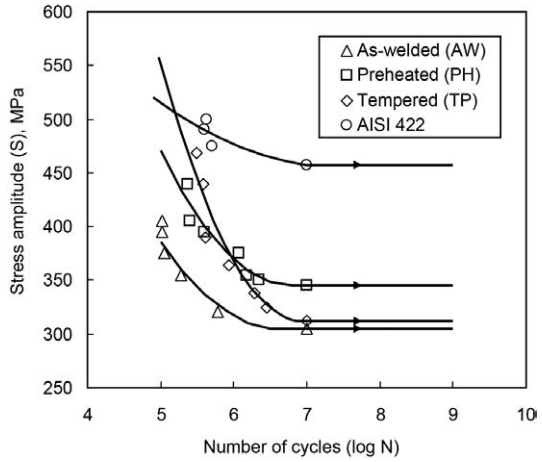

Figure 8: Wöhler (S – N) diagram showing fatigue test results
Slika 8: Wöhlerjeva krivulja (S – N) prikazuje rezultate preizkusov utrujenosti

resulted in a decrease in the YS to 467 MPa. The UTS increased from 630 MPa to 660 MPa with preheating. The tempering further increased the UTS to 683 MPa. The elongation values increased with preheating and tempering treatments. With preheating, the fraction of EL values increased from 12.5 % to 18.8 %. With tempering, the fraction of EL values increased to 25 %.

Table 5: Tensile-test results for the welded AISI 422 alloy for three different heat treatments
Tabela 5: Rezultati nateznih preizkusov varjene AISI 422 zlitine pri treh različnih toplotnih obdelavah

Specimen	Yield strength YS	Ultimate tensile strength UTS	Percent elongation %
AW	490	630	12.5
PH	490	660	18.8
TP	467	683	25.0

The fatigue-test results are given in **Figure 8**. Despite its lower tensile strength (**Figure 5**), the unwelded specimen shows a superior fatigue strength compared to its welded counterparts. The fatigue limit of the unwelded specimen lies at 458 MPa, where the PH, TP and AW specimens display the fatigue limits at (345, 312 and 305) MPa, respectively. These results indicate that the fatigue strength is more dependent on the hardness of a weld. The unwelded specimen is completely martensitic and therefore displays the highest fatigue limit. The AW specimen has the highest hardness among the welded specimens, but it displays the lowest fatigue limit which is probably due to residual stresses. The TP specimen has the lowest hardness distribution among the welded specimens displaying a fatigue limit which is only slightly higher than that of the AW specimen. The PH specimen, on the other hand, displays the highest fatigue limit among the welded specimens, which is due to its moderate hardness and also due to the stress relief provided by the preheating.

4 CONCLUSIONS

The effect of preheating and post-weld tempering on the microstructure and mechanical properties of welded martensitic stainless steels was studied. The conclusions drawn from this study are as follows:

1) The grain boundary precipitation of chromium carbides was observed in the welded joints. The precipitation was mainly caused by the diffusion of carbon into the austenitic stainless steel during the welding.

2) A decrease in the microhardness was observed moving from the base metal to the weld. The decrease in and absence of the martensite phase in the HAZ and the weld, respectively, were the main causes for a decreased hardness.

3) An increase in the tensile strength and percent elongation was observed after the preheating and tempering heat treatments.

4) Preheating provided the best fatigue results for the welded specimens. The fatigue limits observed for the tempered specimens were slightly lower than those found in the preheated specimens.

5 REFERENCES

[1] Welding Handbook, 9th ed., Vol. 1, Welding Science and Technology, American Welding Society, Miami 2007
[2] S. J. Maddox, Recent advances in the fatigue assessment of weld imperfections, Weld. J., 7 (**1992**), 42–50
[3] G. S. Booth, J. G. Wylde, Procedural considerations relating to the fatigue testing of steel weldments, in Fatigue and Fracture Testing of Weldments, ASTM STP 1058, Eds., H. I. McHenry, J. M. Potter, American Society for Testing and Materials, Philadelphia 1990, 3–15
[4] T. N. Nguyen, M. A. Wahab, The effect of weld geometry and residual stresses on the fatigue of welded joints under combined loading, J. Mater. Proc. Technol., 77 (**1998**), 201–208
[5] G. Linnert, Common welding problems: Fatigue, Weld. J., 75 (**1996**), 59–60
[6] A. Ohta, Y. Maeda, N. Suzuki, Fatigue strength of butt-welded joints under constant maximum stress and random minimum stress conditions, Fatigue Fract. Eng. M., 19 (**1996**) 19, 265–275
[7] J. A. Ferreira, C. M. Branco, Fatigue analysis and prediction in fillet welded joints in the low thickness range, Fatigue Fract. Eng. M., 13 (**1990**), 201–212
[8] G. Magudeeswaran, V. Balasubramanian, G. Madhusudhan Reddy, T. S. Balasubramanian, Effect of welding processes and consumables on tensile and impact properties of high strength quenched and tempered steel joints, J. Iron Steel Res. Int., 15 (**2008**), 87–94
[9] L. R. Link, Fatigue crack growth of weldments, in Fatigue and Fracture Testing of Weldments, ASTM STP 1058, Eds., H. I. McHenry, J. M. Potter, American Society for Testing and Materials, Philadelphia 1990, 16–33
[10] M. Ghosh, K. Kumar, R. S. Mishra, Friction stir lap welded advanced high strength steels: Microstructure and mechanical properties, Mater. Sci. Eng., A 528 (**2011**), 8111–8119
[11] ASM Handbook, Vol. 6, Welding, Brazing and Soldering, 2nd ed., Metals Park, ASM International, Ohio 1993
[12] A. J. Williams, P. J. Rieppel, C. B. Voldrich, Literature survey on weld-metal cracking, WADC Technical Report, 52–143, Ohio 1952